

correlation effects and provide a better description of chemical bonds.

Acknowledgment. We are grateful to Prof. John Goddard at Guelph University, Ontario, Canada, Dr. Yoshihiro Osamura

at Keio University, Yokohama, Japan, and Dr. Wesley D. Allen for helpful discussions. This research was supported by the U.S. National Science Foundation, Grant CHE-8718469. M.D. acknowledges the financial support of the Ministerio de Educación y Ciencia of Spain.

Møller–Plesset Perturbation Theory with Spin Projection

H. Bernhard Schlegel*

Department of Chemistry, Wayne State University, Detroit, Michigan 48202 (Received: July 10, 1987; In Final Form: October 23, 1987)

A method has been developed for calculating energies by full spin projection of unrestricted Møller–Plesset perturbation theory wave functions. The spin projection technique has been tested on bond dissociation potentials of LiH and HF and on symmetrically stretched H₂O. In the region where the UHF wave function is more stable than the RHF wave function, spin projected UMP n energies of low order ($n \leq 4$) have smaller errors than the corresponding spin restricted MP n and unprojected UMP n energies, when compared to full configuration interaction calculations. For higher order perturbation theory, spin restricted MP n energies may be more accurate than spin projected UMP n , but only for limited region near the RHF/UHF instability. An approximate spin projected UMP n formalism developed earlier yields energies that are in good agreement with the present full spin projected UMP n calculations. A formula for spin projected energies in the coupled clusters approach is also presented. It is shown that annihilation of any single spin contaminant leaves the CCSD energy unaltered.

Introduction

For open-shell systems, unrestricted Hartree–Fock (UHF)¹ and n th order unrestricted Møller–Plesset perturbation theory (UMP n)^{2,3} are usually quite reliable and yield satisfactory energetics and optimized geometries. However, spin unrestricted wave functions are not eigenfunctions of the \hat{S}^2 operator. This is normally not a significant problem, unless the contamination from higher spin states is large. In such cases, the potential energy surfaces obtained by spin unrestricted methods, such as UHF and UMP n , can be significantly distorted, showing anomalously high barriers for reactions⁴ and bond dissociation potentials that rise too steeply.⁵ These difficulties are due to the extremely slow convergence of unrestricted Møller–Plesset perturbation theory in these regions of the potential energy surface.^{6–8} The convergence difficulties, in turn, can be traced to serious spin contamination in the UHF reference determinant. In a previous paper,⁵ we outlined a simple, approximate scheme to calculate UMP n energies with annihilation of the largest spin contaminant. This method has been used successfully to study some simple bond dissociations⁵ and a number of radical reactions involving additions to multiple bonds,^{4,9–11} isomerizations,¹² and abstractions.¹³ In this paper, we present a method for calculating fully spin projected UMP n energies and give a number of simple examples.

Method

Projected Hartree–Fock Theory. The equations for the projected Hartree–Fock energy are well-known^{14–18} and can be written in terms of the Löwdin spin projection operator.¹⁸

$$E_{\text{proj UHF}} = \langle \hat{P}_s \Psi_0 | \hat{H} | \hat{P}_s \Psi_0 \rangle / \langle \hat{P}_s \Psi_0 | \hat{P}_s \Psi_0 \rangle = \langle \Psi_0 | \hat{H} \hat{P}_s | \Psi_0 \rangle / \langle \Psi_0 | \hat{P}_s | \Psi_0 \rangle \quad (1)$$

$$\hat{P}_s = \prod_{k \neq s} \{ (\hat{S}^2 - k(k+1)) / (s(s+1) - k(k+1)) \} \quad (2)$$

Note that \hat{P}_s is independent and commutes with \hat{H} . The numerator can be expanded by inserting the identity operator, $\hat{I} = |\Psi_0\rangle\langle\Psi_0| + \sum_j |\psi_j\rangle\langle\psi_j|$, where the sum extends over all excited determinants. The projected Hartree–Fock energy and wave function can then be written as

$$E_{\text{proj UHF}} = \langle \Psi_0 | \hat{H} | \Psi_0 \rangle + \sum_i \langle \Psi_0 | \hat{H} | \psi_i \rangle \langle \psi_i | \hat{P}_s | \Psi_0 \rangle / \langle \Psi_0 | \hat{P}_s | \Psi_0 \rangle \quad (3)$$

$$\hat{P}_s \Psi_0 = \Psi_0 + \sum_i |\psi_i\rangle \langle \psi_i | \hat{P}_s | \Psi_0 \rangle / \langle \Psi_0 | \hat{P}_s | \Psi_0 \rangle = \Psi_0 + \tilde{\Psi}_0 \quad (4)$$

Because the UHF wave functions satisfy Brillouin's theorem and \hat{H} contains only one- and two-electron operators, the summation over ψ_i in eq 3 for the projected Hartree–Fock energy can be restricted to all double excitations (but not in eq 4 for the projected wave function).

Approximations to Spin Projected Møller–Plesset Perturbation Theory. Projected Hartree–Fock potential energy curves are known to behave quite poorly in some regions, particularly near

-
- (1) Pople, J. A.; Nesbet, R. K. *J. Chem. Phys.* **1954**, *22*, 571.
 - (2) Møller, C.; Plesset, M. S. *Phys. Rev.* **1934**, *46*, 618.
 - (3) For a review of many-body perturbation theory and coupled cluster methods see: Bartlett, R. J. *Annu. Rev. Phys. Chem.* **1981**, *32*, 359.
 - (4) Sosa, C.; Schlegel, H. B. *Int. J. Quantum Chem.* **1986**, *29*, 1001. **1986**, *30*, 155.
 - (5) Schlegel, H. B. *J. Chem. Phys.* **1986**, *84*, 4530.
 - (6) Handy, N. C.; Knowles, P. J.; Somasundram, K. *Theor. Chim. Acta* **1985**, *68*, 87. Knowles, P. J.; Somasundram, K.; Handy, N. C.; Hirao, K. *Chem. Phys. Lett.* **1985**, *113*, 8.
 - (7) Laidig, W. D.; Fitzgerald, G.; Bartlett, R. J. *Chem. Phys. Lett.* **1985**, *113*, 151.
 - (8) Gill, P. M. W.; Radom, L. *Chem. Phys. Lett.* **1986**, *132*, 16.
 - (9) Sosa, C.; Schlegel, H. B. *J. Am. Chem. Soc.* **1987**, *109*, 4193.
 - (10) Gonzalez, C.; Sosa, C.; Schlegel, H. B., in preparation.
 - (11) Sosa, C.; Schlegel, H. B. *Int. J. Quantum Chem., Quantum Chem. Symp.* **1987**, *21*, 267.
 - (12) Sosa, C.; Schlegel, H. B. *J. Am. Chem. Soc.* **1987**, *109*, 7007.
 - (13) Spin projected UMP n calculations on HO + H₂ → H₂O + H and F + H₂ → HF + H were presented at the 1987 Sanibel Symposium and the 1987 Midwest Theoretical Chemistry Conference. Sosa, C.; Schlegel, H. B. *Chem. Phys. Lett.*, submitted for publication.
 - (14) For a review see: Mayer, I. *Adv. Quantum Chem.* **1980**, *12*, 189.
 - (15) Amos, T.; Hall, G. G. *Proc. R. Soc. London, A* **1961**, *263*, 483. Amos, T.; Snyder, L. C. *J. Chem. Phys.* **1964**, *41*, 1773.
 - (16) Fukutome, *Int. J. Quantum Chem.* **1981**, *21*, 955.
 - (17) Rossky, P. J.; Karplus, M. *J. Chem. Phys.* **1980**, *73*, 6196.
 - (18) Löwdin, P.-O. *Phys. Rev.* **1955**, *97*, 1509.

* Camille and Henry Dreyfus Teacher–Scholar.

the onset of the RHF/UHF instability.¹⁴ As has been demonstrated earlier,^{4,8,9-13} the potential energy curves are much improved when correlation corrections are added to the PUHF results. The spin projection corrections to the UHF wave function and the perturbative corrections to the wave function for electron correlation, Ψ_1 , Ψ_2 , etc., both consist of single, double, and higher excitations. As a first approximation, the spin corrections, $\tilde{\Psi}_0$, must be reduced by the amount already contained in the correlation corrections, Ψ_1 , Ψ_2 , etc. This leads to the following formulas:¹⁹

$$E_{\text{PMP2}} \cong E_{\text{UMP2}} + \Delta E_{\text{PUHF}} \{1 - \langle \tilde{\Psi}_0 | \Psi_1 \rangle / \langle \tilde{\Psi}_0 | \tilde{\Psi}_0 \rangle\} \quad (5a)$$

$$E_{\text{PMP3}} \cong E_{\text{UMP3}} + \Delta E_{\text{PUHF}} \{1 - \langle \tilde{\Psi}_0 | \Psi_1 + \Psi_2 \rangle / \langle \tilde{\Psi}_0 | \tilde{\Psi}_0 \rangle\} \quad (5b)$$

$$E_{\text{PMP4}} \cong E_{\text{UMP4}} + \Delta E_{\text{PUHF}} \{1 - \langle \tilde{\Psi}_0 | \Psi_1 + \Psi_2 + \Psi_3 \rangle / \langle \tilde{\Psi}_0 | \tilde{\Psi}_0 \rangle\} \quad (5c)$$

It can be shown that this approximation goes to the correct limit as the perturbed wave function approaches the exact wave function (i.e., $\langle \tilde{\Psi}_0 | \Psi_1 + \dots + \Psi_\infty \rangle / \langle \tilde{\Psi}_0 | \tilde{\Psi}_0 \rangle = \langle \hat{P}_s \Psi_0 - \Psi_0 | \Psi_{\text{exact}} - \Psi_0 \rangle / \langle \hat{P}_s \Psi_0 - \Psi_0 | \hat{P}_s \Psi_0 - \Psi_0 \rangle = 1$, since $\hat{P}_s \Psi_{\text{exact}} = \Psi_{\text{exact}}$ and \hat{P}_s is idempotent).

If the largest contribution to the spin contamination comes from only the next highest spin, i.e., $s + 1$, it is reasonable to approximate the full projection operator by the first factor in eq 2, $k = s + 1$. However, the resulting operator is no longer a projector (not idempotent) but an annihilation operator, \hat{A}_{s+1} . The operator that destroys all states with spin $s + n$ is given by

$$\hat{A}_{s+n} = \{ \hat{S}^2 + (s+n)(s+n+1) \} / \{ \langle \Psi_0 | \hat{S}^2 | \Psi_0 \rangle - (s+n)(s+n+1) \} \quad (6)$$

where the denominator is chosen to ensure intermediate normalization of $\hat{A}_{s+n} \Psi_0$. Since a single annihilator contains only one- and two-electron operators, the approximation $\hat{P}_s = \hat{A}_{s+1}$ yields a spin correction term, $\tilde{\Psi}_0$ in eq 4, that contains only single and double excitations. This greatly simplifies the computation of the approximate spin projected energies based on eq 5.

Spin Projected Møller-Plesset Perturbation Theory. The approximate spin projected formulas in eq 5 result from the projector or annihilator operating on Ψ_0 only, followed by a correction to avoid double counting of excited configurations already in Ψ_1 , Ψ_2 , etc. Full spin projection would apply the projector to the correlation corrections as well as to Ψ_0 . For UMP n wave functions, the projected energies can be written

$$E_{\text{proj MP2}} = \langle \Psi_0 | \hat{H} | \hat{P}_s \Psi_0 + \hat{P}_s \Psi_1 \rangle / \langle \Psi_0 | \hat{P}_s \Psi_0 + \hat{P}_s \Psi_1 \rangle \quad (7a)$$

$$E_{\text{proj MP3}} = \langle \Psi_0 | \hat{H} | \hat{P}_s \Psi_0 + \hat{P}_s \Psi_1 + \hat{P}_s \Psi_2 \rangle / \langle \Psi_0 | \hat{P}_s \Psi_0 + \hat{P}_s \Psi_1 + \hat{P}_s \Psi_2 \rangle \quad (7b)$$

⋮

The only components of $\hat{P}_s \Psi_1$, $\hat{P}_s \Psi_2$, etc., contributing to the energy are Ψ_0 and the double excitations. This simplifies the computations considerably, and the projected MP n energies can be expressed as

$$E_{\text{proj MP2}} = \langle \Psi_0 | \hat{H} | \Psi_0 \rangle + \sum_i \langle \Psi_0 | \hat{H} | \psi_i \rangle \langle \psi_i | \hat{P}_s | \Psi_0 + \Psi_1 \rangle / \langle \Psi_0 | \hat{P}_s | \Psi_0 + \Psi_1 \rangle \quad (8a)$$

$$E_{\text{proj MP3}} = \langle \Psi_0 | \hat{H} | \Psi_0 \rangle + \sum_i \langle \Psi_0 | \hat{H} | \psi_i \rangle \langle \psi_i | \hat{P}_s | \Psi_0 + \Psi_1 + \Psi_2 \rangle / \langle \Psi_0 | \hat{P}_s | \Psi_0 + \Psi_2 \rangle \quad (8b)$$

⋮

where ψ_i includes all double excitations ($\alpha\alpha$, $\alpha\beta$, $\beta\beta$). To evaluate

$\langle \psi_i | \hat{P}_s | \Psi_1 \rangle$, one needs matrix elements of the type $\langle \psi_i | \hat{S}^{2m} | \psi_j \rangle$, where ψ_i and ψ_j include all double excitations; for $\langle \psi_i | \hat{P}_s | \Psi_2 \rangle$, $\langle \psi_i | \hat{P}_s | \Psi_3 \rangle$, etc., ψ_j must also include higher excitations. For $m = 1$ the matrix is relatively sparse, but for $m > 1$ there are of the order of $n^4 N^4$ nonzero elements between doubly excited determinants, where n is the number of occupied orbitals and N the number of unoccupied orbitals.

A different set of equations for the projected MP n energies can be obtained by taking advantage of the fact that \hat{P}_s and \hat{H} commute.

$$E_{\text{proj MP2}} = [\langle \Psi_0 | \hat{P}_s | \Psi_0 \rangle \langle \Psi_0 | \hat{H} | \Psi_0 + \Psi_1 \rangle + \sum_i \langle \Psi_0 | \hat{P}_s | \psi_i \rangle \langle \psi_i | \hat{H} | \Psi_0 + \Psi_1 \rangle] / \langle \Psi_0 | \hat{P}_s | \Psi_0 + \Psi_1 \rangle \quad (9a)$$

$$E_{\text{proj MP3}} = [\langle \Psi_0 | \hat{P}_s | \Psi_0 \rangle \langle \Psi_0 | \hat{H} | \Psi_0 + \Psi_1 + \Psi_2 \rangle + \sum_i \langle \Psi_0 | \hat{P}_s | \psi_i \rangle \langle \psi_i | \hat{H} | \Psi_0 + \Psi_1 + \Psi_2 \rangle] / \langle \Psi_0 | \hat{P}_s | \Psi_0 + \Psi_1 + \Psi_2 \rangle \quad (9b)$$

⋮

The ψ_i 's run over all single, double, triple, and quadruple excitations in eq 9a, and additionally quintuple and hexuple excitations for eq 9b. The matrix elements $\langle \psi_i | \hat{H} | \Psi_1 \rangle$ are closely related to $|\Psi_2\rangle$ and the MP3 energy; likewise, the $\langle \psi_i | \hat{H} | \Psi_2 \rangle$ are closely related to $|\Psi_3\rangle$ and the MP4 energy. In both approaches considerable factoring should be possible to reduce the work to below $n^4 N^4$. Equation 8 would, at first glance, seem to be more practical, but eq 9 is more amenable to approximations such as limiting the number of spin contaminants to be annihilated or limiting the excited states that appear in the summation. For example, if only the largest spin contaminant is annihilated, i.e., $\hat{P}_s \approx \hat{A}_{s+1}$, then ψ_i runs over single and $\alpha\beta$ type double excitations only.

An alternative formulation of spin projected Møller-Plesset perturbation theory is presented by Knowles and Handy²⁰ elsewhere in this issue. It can be easily shown that the two methods are closely related. If the denominator in eq 7 of the present paper is expanded in a Taylor series, $\langle \Psi_0 | \hat{P}_s | \Psi_0 + \Psi_1 + \Psi_2 + \dots \rangle^{-1} = \langle \Psi_0 | \hat{P}_s | \Psi_0 \rangle^{-1} (1 - \langle \Psi_0 | \hat{P}_s | \Psi_1 + \Psi_2 + \dots \rangle / \langle \Psi_0 | \hat{P}_s | \Psi_0 \rangle + \dots)$, and terms of the same order in \hat{H}_1 are collected, then eq 11 of Knowles and Handy is obtained. For the examples discussed below, the two methods differ in energy by 10^{-3} au or less.

Spin Projected Coupled Cluster Theory. Unrestricted coupled cluster wave functions appear to have less spin contamination than their many-body perturbation theory counterparts.^{21,22} Furthermore, the coupled cluster calculations with singles and doubles (CCSD) describe single bond dissociation potentials quite well.²¹⁻²³ The QCISD method²⁴ seems to have similar properties. This suggests that the CCSD approach and related methods overcome some of the spin contamination problems encountered by unrestricted Møller-Plesset perturbation theory. Analogous to eq 9, the spin projected coupled clusters energy can be written as

$$E_{\text{proj CC}} = [\langle \Psi_0 | \hat{P}_s | \Psi_0 \rangle \langle \Psi_0 | \hat{H} | \Psi_{\text{CC}} \rangle + \sum_i \langle \Psi_0 | \hat{P}_s | \psi_i \rangle \langle \psi_i | \hat{H} | \Psi_{\text{CC}} \rangle] / [\langle \Psi_0 | \hat{P}_s | \Psi_0 \rangle + \sum_j \langle \Psi_0 | \hat{P}_s | \psi_j \rangle \langle \psi_j | \Psi_{\text{CC}} \rangle] \quad (10)$$

The CCSD equations require that $\langle \Psi_0 | \hat{H} | \Psi_{\text{CCSD}} \rangle = E_{\text{CCSD}}$ and $\langle \psi_i | \hat{H} | \Psi_{\text{CCSD}} \rangle = E_{\text{CCSD}} \langle \psi_i | \Psi_{\text{CCSD}} \rangle$ for all single and double excitations.³ Hence, if the summations in the numerator and denominator are restricted to single and double excitations or if \hat{P}_s is restricted to annihilate only one spin contaminant (i.e., if \hat{P}_s is approximated by \hat{A}_{s+n} for any $n \neq 0$, $\langle \Psi_0 | \hat{P}_s | \psi_i \rangle$ is nonzero only for single and double excitations), then the factors in the numerator

(20) Knowles, P. J.; Handy, N. C. *J. Phys. Chem.*, this issue.

(21) Bartlett, R. J.; Sekino, H.; Purvis III, G. D. *Chem. Phys. Lett.* **1983**, *98*, 66.

(22) Cole, S. J.; Bartlett, R. J. *J. Chem. Phys.* **1987**, *86*, 873.

(23) Laidig, W. D.; Saxe, P.; Bartlett, R. J. *J. Chem. Phys.* **1987**, *86*, 887.

(24) Pople, J. A.; Head-Gordon, M.; Raghavachari, K. *J. Chem. Phys.* **1987**, *87*, 5968.

(19) In previous applications the contribution of Ψ_3 to E_{PMP4} was omitted for practical reasons. Furthermore, $\tilde{\Psi}_0$ was restricted to single and double excitations even when the full projector was used. The present calculations indicate that these approximations change the energy by less than 10^{-3} au, except in the immediate vicinity of the RHF/UHF instability.

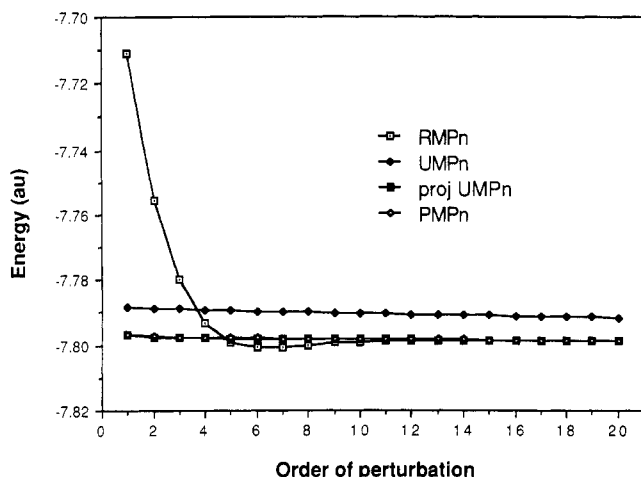


Figure 1. Comparison of convergence rates for restricted, unrestricted, and spin projected unrestricted Møller–Plesset perturbation theory for LiH at $R = 3.0 \text{ \AA}$ (STO-3G basis).

that depend on the projector cancel with the denominator and the coupled cluster energy with single annihilation is identical with the unprojected energy. Thus, CCSD calculations will be sat-

$$E_{\text{CCSD}+sa} = [\langle \Psi_0 | \hat{A}_{s+n} | \Psi_0 \rangle \langle \Psi_0 | \hat{H} | \Psi_{\text{CCSD}} \rangle + \sum_i \langle \Psi_0 | \hat{A}_{s+n} | \psi_i \rangle \langle \psi_i | \hat{H} | \Psi_{\text{CCSD}} \rangle] / [\langle \Psi_0 | \hat{A}_{s+n} | \Psi_0 \rangle + \sum_j \langle \Psi_0 | \hat{A}_{s+n} | \psi_j \rangle \langle \psi_j | \Psi_{\text{CCSD}} \rangle] \quad (11a)$$

$$= [\langle \Psi_0 | \hat{A}_{s+n} | \Psi_0 \rangle E_{\text{CCSD}} + \sum_i \langle \Psi_0 | \hat{A}_{s+n} | \psi_i \rangle \langle \psi_i | \Psi_{\text{CCSD}} \rangle E_{\text{CCSD}}] / [\langle \Psi_0 | \hat{A}_{s+n} | \Psi_0 \rangle + \sum_j \langle \Psi_0 | \hat{A}_{s+n} | \psi_j \rangle \langle \psi_j | \Psi_{\text{CCSD}} \rangle] \quad (11b)$$

$$= E_{\text{CCSD}} \quad (11c)$$

isfactory for problems in which the UHF determinant has only one major spin contaminant, e.g., single-bond dissociation potentials, etc. By the same arguments, processes involving two spin contaminants, e.g., the breaking of two single bonds or the breaking of a double bond, will be treated very well by CCSDTQ. Because of the exponential nature of the coupled clusters wave function, CCSD may be adequate for the breaking of two single bonds, provided they do not interact significantly. A similar approach can be used to show that the QCISD method²⁴ should also be satisfactory for cases with one major spin contaminant.

Results and Discussion

The spin projected UMP n method presented above was tested in the context of a full configuration interaction program. The code for the full CI calculation and the n th-order Møller–Plesset perturbation theory was written by using the approach outlined by Handy et al.²⁵ with the formula list organized as suggested by Siegbahn.²⁶ Details will be published elsewhere. A number of simple examples have been studied to compare RMP n , UMP n , and projected UMP n with full configuration interaction calculations and to test various approximations. The spin projected UMP n energies were calculated according to eq 9 and the PMP n energies according to eq 5. The full spin projector, \hat{P}_s , was used throughout, and no restrictions were placed on the sums over excited states.

In the first example, the bond dissociation curve for LiH has been computed with the STO-3G basis set. Calculations were performed with restricted, unrestricted, and spin projected unrestricted Møller–Plesset perturbation theory up to 20th order and with full configuration interaction (six active orbitals). Figure 1 shows the rate of convergence of the various levels at a bond

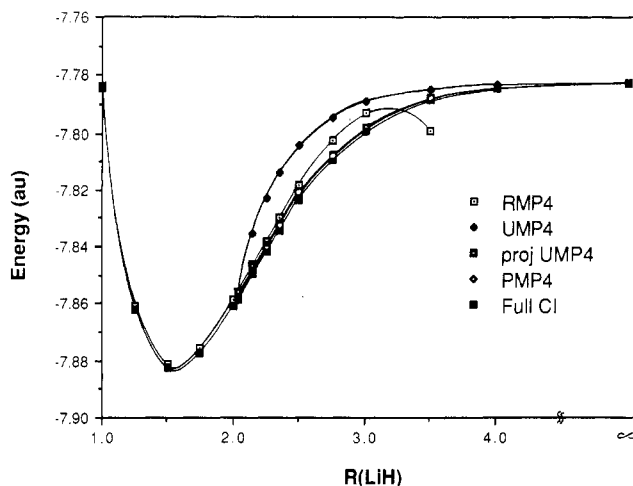


Figure 2. Bond dissociation potential for LiH at the MP4 level (STO-3G basis).

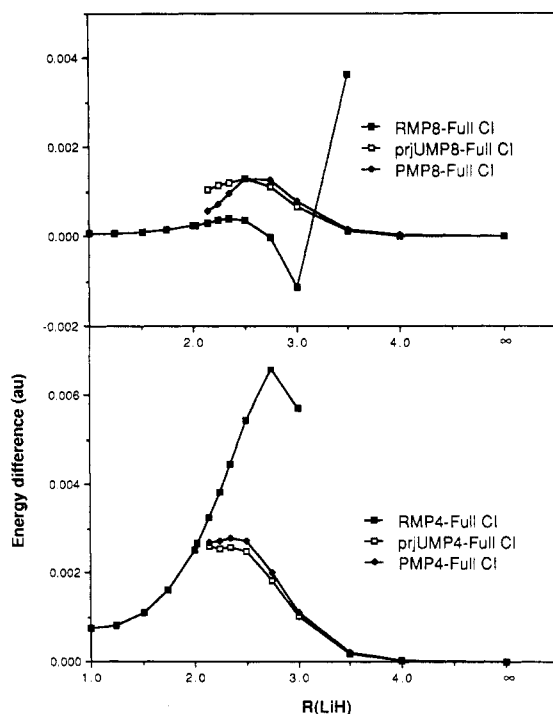


Figure 3. Energy difference between MP4, MP8, and full CI as a function of bond length for LiH (STO-3G basis).

length of 3 \AA . As has been pointed out previously,^{6–8} the UMP n series is very slow to converge. The RMP n series converges more rapidly than the unprojected UMP n series but undergoes oscillations that become quite severe at longer bond lengths. Since the practical limit for larger molecules is MP4, it is instructive to examine the behavior of the dissociation curve computed with the various approaches at fourth order. Figure 2 illustrates the potential energy curves at the various levels, and Figure 3 shows the difference between the restricted, unrestricted, and spin projected MP4 and MP8 energies and the full CI energy. The UMP4 curve rises too steeply in the intermediate region, and the RMP4 curve turns over beyond 3 \AA . The difference between the projected UMP4 and the full CI energies is largest (ca. 1.5 kcal/mol) near the onset of the RHF/UHF instability but diminishes rapidly for increasing bond lengths. Beyond the RHF/UHF instability ($R > 2.0334 \text{ \AA}$), the difference between the projected UMP4 and full CI energies is less than the difference between RMP4 and full CI. The approximate projected UMP4 approach (PMP4) used earlier is in very good agreement with the fully projected UMP4 energies at all bond lengths. For eighth-order perturbation theory, the restricted MP curve is more accurate

(25) Knowles, P. J.; Handy, N. C. *Chem. Phys. Lett.* **1984**, *111*, 315.

(26) Siegbahn, P. E. M. *Chem. Phys. Lett.* **1984**, *109*, 417.

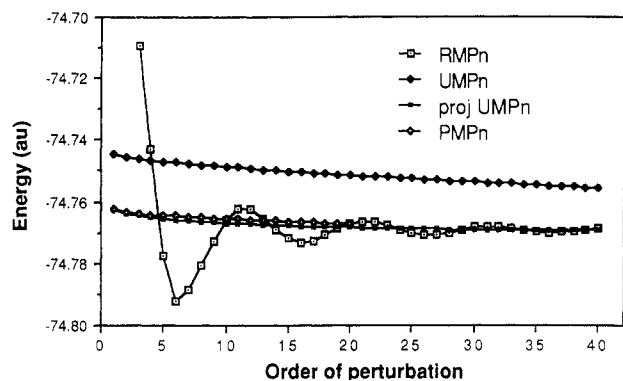


Figure 4. Comparison of convergence rates for restricted, unrestricted, and spin projected unrestricted Møller-Plesset perturbation theory for symmetrically stretched H_2O at $R = 1.934 \text{ \AA}$ (STO-3G basis).

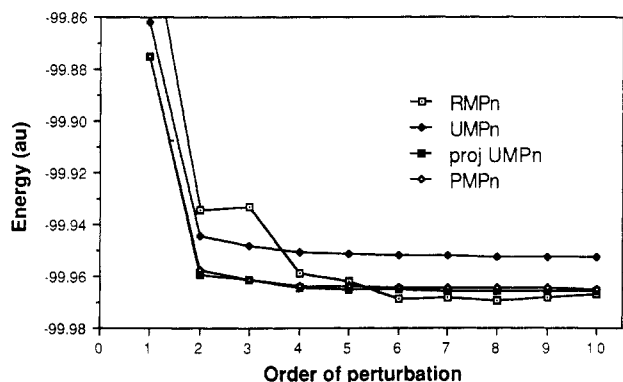


Figure 5. Comparison of convergence rates for restricted, unrestricted, and spin projected unrestricted Møller-Plesset perturbation theory for HF at $R = 2.0 \text{ \AA}$ (6-31G basis).

up to ca. 2.75 \AA ; however, for longer distances the spin projected UMP is superior.

The second example considered is H_2O with both bonds stretched to twice the equilibrium value ($R = 1.934 \text{ \AA}$). Calculations were performed with the STO-3G basis set using restricted, unrestricted, and spin projected unrestricted Møller-Plesset perturbation theory up to 40th order, as well as full configuration interaction (frozen core). Spin contamination from both the triplet and quintet²⁷ must be removed for meaningful results with eq 5, 8, or 9. Figure 4 shows the rate of convergence of the various levels. Similar to LiH, the RMP n series oscillates and UMP n series converges very slowly. The projected UMP n series lies much closer to the full CI result but retains a small, slowly converging component. The approximate PMP n energies are in very good agreement with the fully projected UMP n energies.

In the third example, the bond dissociation curve for HF has been calculated with the 6-31G basis set using Møller-Plesset perturbation theory up to 10th order and full configuration interaction (frozen core). Contamination from spin states higher than the quintet contribute less than 2×10^{-6} au to the energy. As shown in Figure 5, the rate of convergence of the RMP n series at $R(\text{HF}) = 2.0 \text{ \AA}$ is considerably more erratic than for the minimal basis set calculations discussed above. Similar erratic behavior has been noted for double- ζ basis set RMP n calculations on symmetrically stretched H_2O .²¹ The convergence of the UMP n series is slow but monotonic. Up to fourth order, the projected UMP n series converges rapidly to within 0.002 au of the full CI result; beyond fourth order the rate of convergence is considerably slower. The approximate PMP n values are in good agreement with the results of full spin projection. Figure 6 illustrates the HF bond dissociation potential calculated at the RMP4, UMP4, projected UMP4, PMP4, and full CI levels; differences between the MP4, MP8, and full CI energies are given in Figure 7. The behavior is very similar to LiH. The difference between the

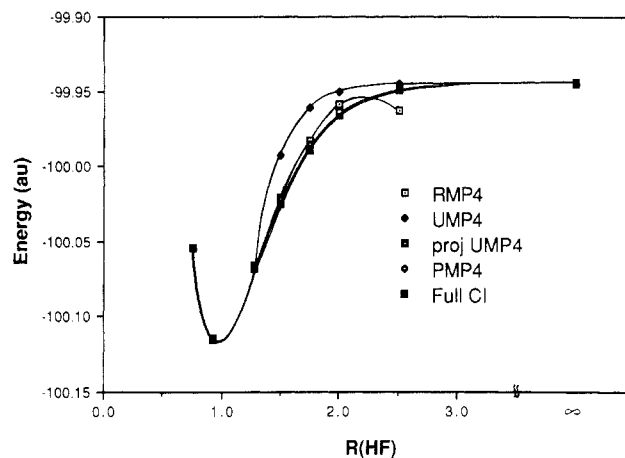


Figure 6. Bond dissociation potential for HF at the MP4 level (6-31G basis).

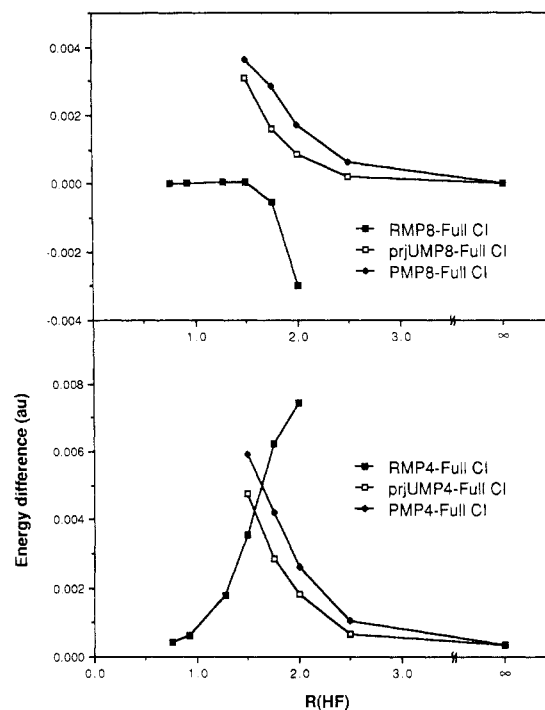


Figure 7. Energy difference between MP4, MP8, and full CI as a function of bond length for HF (6-31G basis).

projected UMP4 and full CI energies is largest near the RHF/UHF instability ($R = 1.2771 \text{ \AA}$). At eighth order, the RMP energy is better than the projected UMP energy up to $R = 1.75 \text{ \AA}$. However, for longer bond lengths, the error in the projected UMP n energies is less than the error for RMP n . The approximate PMP4 energies are in good agreement with the projected UMP4 energies, especially at larger distances.

Conclusions

A formalism for calculating spin projected UMP n energies has been proposed, and test calculations were carried out for LiH, H_2O , and HF. For low orders ($n \leq 4$), spin projected UMP n energies are better than RMP n and unprojected UMP n energies. Higher order RMP n energies may be more accurate than spin projected UMP n , but only for a short distance beyond the onset of the RHF/UHF instability. The approximate spin projected UMP n (PMP n) method used in earlier calculations is in good agreement with the full spin projected UMP n computations. Spin projection can also be applied to the spin unrestricted coupled clusters method. It is shown that the CCSD energy is unaltered by the annihilation of any single spin contaminant.

Acknowledgment. This work was supported by a grant from the National Science Foundation.

(27) Higher spin states are not possible because of the basis set size.